# A SIMPLE NUMERICAL METHOD FOR CALCULATING GAUSSIAN NMR SPECTRAL LINE SHAPES PARTIALLY NARROWED DUE TO A MOTION WITH THE EXPONENTIAL SPECTRAL AUTOCORRELATION FUNCTION

Jaromír JAKEŠ

*Institute of Macromolecular Chemistry, Academy of Sciences of the Czech Republic, Heyrovského nám. 2, 162 06 Prague 6, Czech Republic; e-mail: jakes@imc.cas.cz*

Received April 17, 2001
Accepted December 3, 2001

A simple numerical method for calculating NMR spectral line shapes resulting from a Gaussian line by a partial narrowing due to a motion with the exponential spectral autocorrelation function of the form exp $(-|\tau|/\tau_c)$ was developed. It was found that the partially narrowed line is narrower not only than the parent Gaussian line with the second moment of $\omega_p^2$ but also than the Lorentzian line with the half-width of $2\omega_p^2\tau_c$ obtained from the extreme narrowing approximation. The central intensity increase compared with the closer of these two lines is less than 50.2%. Asymptotic developments for large values of $\omega - \omega_0$ and for large values of $\omega_p\tau_c$ were derived. Two-term approximation applied to the extreme narrowing case led to a very simple modification of the Lorentzian line having the correct second moment $\omega_p^2$. Analysis of this modified Lorentzian line showed that attempts to estimate $\omega_p^2$ from truncated second moments of Lorentzian lines without knowledge of $\tau_c$ are hopeless. The case of the polyexponential spectral autocorrelation function with all but one correlation times fast enough to allow for the extreme narrowing, modelling the case of an anisotropic motion, is also considered.

**Keywords**: NMR spectroscopy; NMR line shape calculation; Partial motional narrowing of Gaussian line; Exponential spectral autocorrelation function; Second moment; Anisotropic motion.

In a recent study of NMR spectra of poly(2-ethylhexyl acrylate)-*block*-poly(acrylic acid) micelles in water[1], multiexponential relaxation of transverse magnetization with a peculiar behaviour of $T_2$ relaxation times was observed. Since a narrowing of spectral lines in magic angle spinning was observed simultaneously[1], it was assumed that incomplete averaging of the dipole–dipole interactions due to a motion not fast enough was responsible. Hence, it was worth performing a more detailed study of the calculation of the line shapes of partially narrowed NMR spectral lines.


doi:10.1135/cccc20020405

The problem of motional and exchange narrowing of NMR and EPR spectral lines was extensively studied by Anderson and Weiss[2] and by Anderson[3]. For a very fast motion, a simple Lorentzian line (the narrower the faster was the motion) resulted. For every speed of the motion, a simple result was obtained also for the Gaussian spectral line, where the narrowed line shape was shown to depend only on the spectral autocorrelation function $\varphi_{\Delta\omega}(\tau)$

$$\varphi_{\Delta\omega}(\tau) = \overline{\left(\omega(t) - \omega_0\right)\left(\omega(t+\tau) - \omega_0\right)} \,/\, \overline{\left(\omega(t) - \omega_0\right)^2} \,. \qquad (1)$$

With this spectral autocorrelation function, the Fourier transform $\varphi(\tau)$ of the narrowed Gaussian line becomes

$$\varphi(\tau) = \exp\,(-\omega_p^2 \int_0^\tau \varphi_{\Delta\omega}(x)(\tau - x)\,\mathrm{d}x)\,, \qquad (2)$$

where $\omega_p^2$ is the second moment of the Gaussian line being narrowed. Anderson further considered two examples of the spectral autocorrelation function, the exponential one, $\varphi_{\Delta\omega}(\tau) = \exp\,(-|\tau|/\tau_c)$, suitable for a Markovian motion, and the Gaussian one, $\varphi_{\Delta\omega}(\tau) = \exp\,(-\pi\tau^2/(4\tau_c^2))$, which may simulate the case where the possible rate of the frequency change is severely limited[3] (exchange narrowing). For the latter spectral autocorrelation function, an approximate calculation of the central intensity and half-width of the narrowed line in the intermediate region (*i.e.*, around $\omega_p\tau_c = 1$) was given in Appendix III of the paper[3]. On the other hand, the former spectral autocorrelation function is more appropriate for a motional narrowing. Therefore, it was worth considering more thoroughly the motional line narrowing with the exponential spectral autocorrelation function. Fortunately, it was possible to develop a simple numerical method for calculating narrowed line shapes in this case, avoiding numerical Fourier transform, which enabled an easy calculation of spectral lines and a detailed analysis of their behaviour in some limiting cases. The results of this consideration are reported in the present paper.

## MATHEMATICAL METHODS

According to Eq. (*36*) of ref.[3], the Fourier transform $\varphi(\tau)$ of the Gaussian spectral line with the second moment $\omega_p^2$ narrowed due to a motion with the exponential spectral autocorrelation function $\varphi_{\Delta\omega}(\tau) = \exp(-|\tau|/\tau_c)$ is given by

$$\varphi(\tau) = \exp(\omega_p^2 \tau_c^2 [1 - |\tau|/\tau_c - \exp(-|\tau|/\tau_c)]). \tag{3}$$

Inverting the Fourier transform, we obtain for the spectral line intensity

$$I(\omega) = \int_{-\infty}^{\infty} \exp(-i(\omega - \omega_0)\tau) \exp(\omega_p^2 \tau_c^2 [1 - |\tau|/\tau_c - \exp(-|\tau|/\tau_c)])\, d\tau / (2\pi), \tag{4}$$

where $\omega_0$ is the center of the spectral line. Due to the symmetry of the function $\varphi(\tau)$, Eq. (*4*) can further be rewritten in the form

$$I(\omega) = \mathrm{Re}[\int_0^{\infty} \exp(-i(\omega - \omega_0)\tau + \omega_p^2 \tau_c^2 [1 - \tau/\tau_c - \exp(-\tau/\tau_c)])\, d\tau]/\pi, \tag{5}$$

where Re means the real part of the expression in the brackets. Note that taking in Eq. (*5*) the imaginary part instead of the real one gives the dispersion component of the narrowed line. To solve the integral in Eq. (*5*), we use the substitution $\omega_p^2 \tau_c^2 \exp(-\tau/\tau_c) = z$, hence $\tau = -\tau_c \ln(z/\omega_p^2 \tau_c^2)$, $d\tau = -\tau_c\, dz/z$. After some rearrangements, we obtain

$$I(\omega) = \tau_c \mathrm{Re}[(\omega_p^2 \tau_c^2)^{-\omega_p^2 \tau_c^2 - i(\omega - \omega_0)\tau_c} \exp(\omega_p^2 \tau_c^2) \gamma(\omega_p^2 \tau_c^2 + i(\omega - \omega_0)\tau_c, \omega_p^2 \tau_c^2)]/\pi,$$

where $\gamma(a, x) = \int_0^x z^{a-1} \exp(-z)\, dz$ is the incomplete gamma function. Now, combining Eqs (*6.5.4*) and (*6.5.29*) of ref.[4], we have

$$\gamma(a, x) = x^a \exp(-x) \sum_{n=0}^{\infty} (x^n \Gamma(a) / \Gamma(a + n + 1)) = x^a \exp(-x) \sum_{n=0}^{\infty} (x^n / \prod_{k=0}^{n} (a + k)),$$

where $\Gamma(t) = \int_0^{\infty} u^{t-1} \exp(-u)\, du$ is the complete gamma function. Replacing the incomplete gamma function by the above series gives the final result

$$I(\omega) = \tau_c \mathrm{Re}[\sum_{n=0}^{\infty} ((\omega_p^2 \tau_c^2)^n / \prod_{k=0}^{n} (\omega_p^2 \tau_c^2 + i(\omega - \omega_0)\tau_c + k))]/\pi \tag{6}$$

or, if we set $\omega_p^2 \tau_c^2 = x$, $(\omega - \omega_0)\tau_c = y$,

$$I(\omega) = \tau_c \, \mathrm{Re}[\sum_{n=0}^{\infty} (x^n / \prod_{k=0}^{n} (x + \mathrm{i}y + k))] / \pi . \tag{6a}$$

In considering convergence properties of the series (*6a*), we can see that for a real $y$ and a real positive $x$, replacing $y$ with zero increases the absolute value of every term of the series, as it leads to a decrease in the absolute value of each factor of the product in the denominator. Hence, the series

$$\sum_{n=0}^{\infty} a_n = \sum_{n=0}^{\infty} (x^n / \prod_{k=0}^{n} (x + k)) \tag{7}$$

is a majorant to the series in Eq. (*6a*) with the same real positive $x$ and any real $y$. Now, starting with some $n_0$, the series (*7*) itself has a majorant $a_{n_0}(x/(x + n_0))^{n-n_0}$, which is a convergent geometric series. From its known sum we see that the error made by terminating the series (*7*) at $n = n_0$ is less than $a_{n_0} x/n_0$. So, the series (*7*), and hence also the series in Eq. (*6a*), both converge for every real positive $x$ and real $y$. For large $x$, the series still converge without loss of accuracy; however, the convergence is slow. For example, for $x$ = 10 000 (*i.e.*, $\omega_p\tau_c = 100$), about 700 terms are necessary to get $a_n < 10^{-13}$, the error in the sum is then less than $1.5 \cdot 10^{-12}$.

In the case of a fast motion (*i.e.*, small $\tau_c$), the value of $x$ is small so that a few of the first terms of the series (*6a*) are sufficient to obtain full convergence. Taking the first term, we obtain

$$I(\omega) = \tau_c x / (\pi(x^2 + y^2)) = \omega_p^2 \tau_c / (\pi(\omega_p^4 \tau_c^2 + (\omega - \omega_0)^2)) , \tag{8}$$

which is the well-known Lorentzian line of the half-width of $2\omega_p^2\tau_c$ for the case of extreme narrowing. We can see that the second term of the series (*6a*) contains in its real part the value of $x$ in the same (first) power as the first term does, and only the third and next terms contain only higher powers of $x$. So, in considering the limiting case $x \to 0$ two first terms should be considered:

$$\begin{aligned} I(\omega) &= \tau_c \, \mathrm{Re}[(x / (x + 1 + \mathrm{i}y) + 1) / (x + \mathrm{i}y)] / \pi = \\ &= \tau_c x(x + 1)(2x + 1) / (\pi(x^2 + y^2)((x + 1)^2 + y^2)) \doteq \\ &\doteq [\tau_c x / (\pi(x^2 + y^2))] \times 1 / (1 + y^2) . \end{aligned} \tag{9}$$

In the last step, $x$ was neglected compared with unity. The last expression in Eq. (*9*) is not exactly normalized, its normalization can be achieved by multiplying it by the factor $1 + x$. Then we obtain

$$I(\omega) = [\tau_c x / (\pi(x^2 + y^2))] \times (1 + x) / (1 + y^2) =$$

$$= [\omega_p^2 \tau_c / (\pi(\omega_p^4 \tau_c^2 + (\omega - \omega_0)^2))] \times (1 + \omega_p^2 \tau_c^2) / (1 + (\omega - \omega_0)^2 \tau_c^2). \qquad (10)$$

The last factor in Eq. (*10*) may be looked on as a correction to the Lorentzian line (*8*). With this correction, the line is exactly normalized and its second moment is exactly $\omega_p^2$ as it should be. The correction factor may become important for $\omega - \omega_0 = \pm 1/(10\tau_c)$, where it decreases the intensity by about 1%, and for larger $|\omega - \omega_0|$, where the intensity decreases more, and eventually, the $(\omega - \omega_0)^{-4}$ decrease is obtained for $|\omega - \omega_0| > 10/\tau_c$ compared with the $(\omega - \omega_0)^{-2}$ decrease in the uncorrected Lorentzian line. The increase caused by the numerator is quite negligible and the second term in the numerator was introduced just to obtain the exact normalization. It is quite clear that in the usual case of the thermal motion, where $\tau_c$ is about $10^{-6}$–$10^{-8}$ s, the correction might be seen only for $|\omega - \omega_0| > 10^5$ s$^{-1}$, *i.e.*, very far beyond the spectral region measured. This means that any attempts made in the past to introduce some truncated second moments of the Lorentzian line are quite arbitrary and cannot lead to the value of $\omega_p^2$, which only may be estimated if we have an at least rough estimate of $\tau_c$.

The case of the slow motion (large $\tau_c$) cannot be treated as easily as the fast motion. Its discussion is done in the subsequent paragraph where the asymptotic developments for large $\tau_c$ and for large $|\omega - \omega_0|$ are considered.

Equation (*6a*) calculates the central intensity of the narrowed line without any loss of accuracy and other points with the same absolute accuracy. However, in far wings, a considerable loss of the relative accuracy occurs, since the leading terms of both the first two members of the sum in Eq. (*6a*) decrease with $y^{-2}$ and these terms cancel yielding the $y^{-4}$ decrease in the result. This can be avoided by summing up the first two members of the sum analytically as in Eq. (*9*); however, even then, some loss of accuracy persists in far wings at large $x$, since the leading term of Eq. (*9*) is $\tau_c x(x + 1)(2x + 1)/(\pi y^4)$, whereas that of Eq. (*6a*) is $\tau_c x/(\pi y^4)$. This drawback can be avoided as follows; at this, complex numbers arithmetic appearing in Eq. (*6a*) is removed as well.

We start from the identity

$$1/\prod_{k=0}^{j}(x+k+\mathrm{i}y) = \sum_{i=[j/2]}^{j}(-1)^{j-i}[(x+i)(\binom{i+1}{j-i}+\binom{i}{j-i-1}) - \\ -\mathrm{i}y\binom{i}{j-i}]\prod_{k=j}^{2i-1}(2x+k)/\prod_{k=0}^{i}((x+k)^2+y^2) \qquad (11)$$

(for $j = 2i + 1$, $\prod_{k=j}^{2i-1}(2x+k) = 1/(2x + 2i)$ and $\binom{i}{j-i} = 0$ should be set, and also $\binom{i}{j-i-1} = 0$ for $j = i$). Now

$$(x+i)\prod_{k=j}^{2i-1}(2x+k) = \sum_{k=0}^{2i+1-j}2^{k-1}S_{2i+1-j-k}(j-1, 2i)x^k\ , \qquad (12)$$

where $S_k(j, i)$, $j \le i$, is the $k$-th symmetric form of the subsequent integers from $j$ + l to $i$. There is $S_0(j, i) = 1$, $S_k(i, i) = 0$ for $k > 0$, and

$$S_k(j-1, i) = S_k(j, i) + jS_{k-1}(j, i)\,. \qquad (13)$$

Herefrom, $S_1(j, i) = (i-j)(i+j+1)/2$, $S_2(j, i) = (i-j)(i-j-1)(3(i+j)^2 + 5i + 7j + 2)/24$, and so forth. Introducing Eq. (*11*) into Eq. (*6a*) and summing up with respect to $j$ at constant $i$ yields

$$I(\omega) = \tau_c(\sum_{n=1}^{\infty}[x^n U_n(x)/\prod_{k=0}^{n}((x+k)^2+y^2)])/\pi\ , \qquad (14)$$

where $U_n(x) = nx^{n-1} + n(n-1)(n+4)x^{n-2} + n(n-1)(n-2)(3n^2 + 25n + 78)x^{n-3}/6$ + ... are polynomials of $x$ with positive integer coefficients. Obtaining next coefficients in a closed form is cumbersome; they can be calculated by numerical summation with respect to $j$ using Eq. (*13*) in calculating $S_k(j, i)$. At this, great loss of accuracy occurs at large $n$'s, so that the calculation should be performed to full accuracy with multiple-precision integer arithmetic for such $n$'s.

The series in Eq. (*14*) needs more (about twice) terms than in Eq. (*6a*) to converge; however, due to the absence of the complex numbers arithmetic, the calculation of the line shape by Eq. (*14*) is still faster than that by Eq. (*6a*) when $x^nU_n(x)$ and $(x + k)^2$ values are precalculated once for all values of $y$. No loss of accuracy occurs since all terms involved are positive.

*Asymptotic Developments*

To obtain asymptotic behaviour of the narrowed line for large $\tau_c$ and for large $|\omega - \omega_0|$, we need the asymptotic developments of the function $\gamma(x + y, x)$ for large positive $x$ and for large pure imaginary $y$. Furch[5] studied the asymptotic behaviour of the function $\Gamma(\alpha, x) = \Gamma(\alpha) - \gamma(\alpha, x)$ and found an asymptotic development for the function $\Gamma(\alpha + 1, \alpha + x)$ for large $\alpha$ (his $n - 1$) and small $x$ (his $1 - \alpha$). Tricomi[6] later derived the asymptotic development for the function $\gamma(\alpha + 1, \alpha + x)$ for large $\alpha$ in terms of $\alpha$ and of the value $x(2\alpha)^{-1/2}$ and also for the function $\Gamma(\alpha + 1, x)$ for both $\alpha$ and $x$ large, so that $x - \alpha$ is large compared with $\alpha^{1/2}$, in terms of $\alpha$ and $x - \alpha$. For large $y$, the series in Eq. (*6a*) is itself asymptotic; however, obtaining from it a series in negative powers of $y$ is very laborious. Due to this fact and also as we need a development of $\gamma(\alpha, x)$ in terms of $x$ and $\alpha - x$ rather than existing developments in terms of $\alpha - 1$ and $x - \alpha + 1$, we use an alternative method for deriving the desired asymptotic developments.

We consider the function

$$f(x, y) = x^{-x-y} \exp(x)\gamma(x + y, x) = x^{-x-y} \exp(x)\int_0^x z^{x+y-1} \exp(-z)\,\mathrm{d}z\,. \qquad (15)$$

Then $I(\omega) = \tau_c \operatorname{Re}[f(\omega_p^2 \tau_c^2, \mathrm{i}(\omega - \omega_0)\tau_c)]/\pi$. Using the substitution $z = x \exp(-\tau)$, we find that

$$f(x, y) = \int_0^\infty \exp(-\tau y)\exp(x[1 - \tau - \exp(-\tau)])\,\mathrm{d}\tau =$$
$$= \int_0^\infty \exp(-\tau y)\exp(-x\tau^2/2) \times \exp(x[1 - \tau + \tau^2/2 - \exp(-\tau)])\,\mathrm{d}\tau\,. \qquad (16)$$

Expanding the last factor into the Taylor series with respect to $x$, we get the expression $1 + \sum_{n=1}^{\infty} x^n T_n(\tau)$, where $T_n(\tau) = (1 - \tau + \tau^2/2 - \exp(-\tau))^n / n!$. Taking the derivative of $T_n$ with respect to $\tau$, we find $\mathrm{d}T_n(\tau)/\mathrm{d}\tau = -nT_n(\tau) + \tau^2 T_{n-1}(\tau)/2$, $T_0(\tau) = 1$. We further expand $T_n(\tau)$ into the Taylor series,

$T_n(\tau) = \sum_{k=3n}^{\infty} (-1)^{k+n} a_{n,k} \tau^k / k!$ and substitute this expansion into the expression for $\mathrm{d}T_n(\tau)/\mathrm{d}\tau$. Comparing coefficients at $\tau^k$, we find that

$$a_{n,k+1} = n a_{n,k} + k(k-1) a_{n-1,k-2} / 2 \qquad (17)$$

for $n > 0$ and $k > 3n$. Further $a_{0,0} = 1$, $a_{0,k} = 0$ for $k > 0$, $a_{n,k} = 0$ for $k < 3n$, and $a_{n,3n} = (3n - 1)(3n - 2)a_{n-1,3n-3}/2 = (3n)!/(n!6^n)$. From Eq. (*17*) it follows, that all nonzero $a_{n,k}$ are positive integers, $a_{1,k} = 1$ for $k > 2$, the values of $a_{2,k}$ starting from $k = 6$ are 10, 35, 91, 210, 456, 957, 1 969 ($2^{k-1} - k(k + 1)/2 - 1$), of $a_{3,k}$ starting from $k = 9$ they are 280, 2 100, 10 395, 42 735, $a_{4,12} = 15\,400$. Then Eq. (*16*) becomes

$$f(x, y) = \int_0^{\infty} \exp(-\tau y) \exp(-x\tau^2 / 2)\Big(1 + \sum_{n=1}^{\infty} x^n \sum_{k=3n}^{\infty} (-1)^{k+n} a_{n,k} \tau^k / k!\Big)\, \mathrm{d}\tau . \qquad (18)$$

Using the substitution $\tau = u/x^{1/2}$, the double series in Eq. (*18*) becomes

$$\sum_{n=1}^{\infty} \sum_{k=3n}^{\infty} (-1)^{k+n} u^k x^{n-k/2} a_{n,k} / k! = \sum_{k=1}^{\infty} x^{-k/2} \sum_{n=1}^{k} (-1)^n a_{n,k+2n} (-u)^{k+2n} / (k+2n)!;$$

the latter expression is obtained from the former by using a new summation variable $k - 2n$ instead of the $k$ (and denoting it again $k$) and by interchanging the order of summation. So,

$$f(x, y) = x^{-1/2} \int_0^{\infty} \exp(-u(y / x^{1/2}) - u^2 / 2)\Big(1 + \sum_{k=1}^{\infty} x^{-k/2} \sum_{n=1}^{k} (-1)^n a_{n,k+2n} (-u)^{k+2n} / (k+2n)!\Big)\, \mathrm{d}u . \qquad (19)$$

Now,

$$\int_0^{\infty} (-u)^r \exp(-uv - u^2 / 2)\, \mathrm{d}u = \mathrm{d}^r((\pi / 2)^{1/2} \exp(v^2 / 2) \operatorname{erfc}(v / 2^{1/2})) / \mathrm{d}v^r = (\pi / 2)^{1/2} \exp(v^2 / 2) \operatorname{erfc}(v / 2^{1/2}) R_r(v) + S_r(v) , \qquad (20)$$

where $\operatorname{erfc}(x) = (2/\pi^{1/2})\int_x^{\infty} \exp(-t^2)\,\mathrm{d}t$, $R_0(v) = 1$, $S_0(v) = 0$, $R_{r+1}(v) = \mathrm{d}R_r(v)/\mathrm{d}v + vR_r(v)$, $S_{r+1}(v) = \mathrm{d}S_r(v)/\mathrm{d}v - R_r(v)$. The recursive formulae for $R_r(v)$ and $S_r(v)$

are derived by applying the d/d$v$ operator to Eq. (*20*). From these formulae follows: $R_r(v)$ is a polynomial of degree $r$, which is even (contains only even powers of $v$) if $r$ is even and odd if $r$ is odd; $S_r(v)$ is a polynomial of degree $r - 1$, which is odd if $r$ is even and even if $r$ is odd. Note that $R_r(v) = \mathrm{i}^{-r} 2^{-r/2} \mathrm{H}_r(\mathrm{i}v / 2^{1/2})$, where $\mathrm{H}_r$ is the Hermite polynomial of degree $r$. Using Eq. (*20*) in Eq. (*19*), we obtain eventually

$$f(x, y) = \sum_{n=0}^{\infty}((\pi / 2)^{1/2} \exp (y^2 / (2x)) \operatorname{erfc} (y / (2x)^{1/2}) P_n(y / x^{1/2}) + \\ + Q_n(y / x^{1/2})) / x^{(n+1)/2} , \qquad (21)$$

where $P_0(v) = 1$, $Q_0(v) = 0$,

$P_n(v) = \sum_{k=1}^{n}(-1)^k a_{k,n+2k} R_{n+2k}(v) / (n + 2k)!$,

$Q_n(v) = \sum_{k=1}^{n}(-1)^k a_{k,n+2k} S_{n+2k}(v) / (n + 2k)!$. The series (*21*) is divergent; however, at least for large positive $x$ and complex $y$ with a non-negative real part, it is a good asymptotic development for $f(x, y)$. $P_n(v)$ is a polynomial of degree $3n$ and its parity is the same as that of $n$, whereas $Q_n(v)$ is a polynomial of degree $3n - 1$ and of the parity opposite to that of $n$. Calculating $P_n(v)$ and $Q_n(v)$ from expressions following Eq. (*21*) is a rather laborious task and a considerable loss of accuracy occurs in performing indicated sums for higher $n$. Fortunately, it was possible to derive much simpler expressions for $P_n(v)$ and $Q_n(v)$ shown below.

Taking in Eq. (*15*) partial derivatives with respect to $x$ and $y$, we easily find that

$$x(f_x - f_y) + yf = 1. \qquad (22)$$

We further introduce the function $g(x, y) = f(x, y) \exp (-y^2/(2x))$. Substituting

$$f = g \exp (y^2 / (2x)) \qquad (23)$$

into Eq. (*22*), we find further

$$x(g_x - g_y) - y^2 g/(2x) = \exp(-y^2/(2x)) . \qquad (24)$$

Considering that exp ($v^2$) erfc ($v$) = $\sum_{n=0}^{\infty}(-v)^n / \Gamma(n/2+1)$, we see that Eq. (*21*) can be rewritten in the form

$$f(x,y) = \sum_{n=0}^{\infty}\sum_{k=0}^{\infty} f_{n,k} y^k / x^{(n+k+1)/2} . \qquad (25)$$

Substituting Eq. (*25*) into Eq. (*22*) and comparing coefficients at $y^k/x^{(n+k+1)/2}$, we find $-(n + k + 1)f_{n,k}/2 - (k + 1)f_{n+1,k+1} + f_{n+1,k-1} = \delta_k\delta_{n+1}$ provided we set $f_{n,k} = 0$ for $k < 0$ and for $n < 0$. Hence

$$\begin{aligned} f_{0,1} &= -1, \quad f_{n+1,1} = -(n+1)f_{n,0}/2 \quad \text{for } n \geq 0 , \\ f_{n+1,k+1} &= (-(n+k+1)f_{n,k}/2 + f_{n+1,k-1})/(k+1) \quad \text{for } k > 0, n \geq 0 , \qquad (26) \\ f_{0,k+2} &= f_{0,k}/(k+2) \quad \text{for } k \geq 0 . \end{aligned}$$

Provided the coefficients $f_{n,0}$ are known from another source, Eq. (*26*) is a simple recursive formula for calculating coefficients $f_{n,k}$ by increasing $n$ by one. Two different methods of obtaining $f_{n,0}$ are given below. Comparing Eqs (*25*) and (*21*), we further see that

$$(\pi/2)^{1/2} \exp(v^2/2) \operatorname{erfc}(v/2^{1/2}) P_n(v) + Q_n(v) = \sum_{k=0}^{\infty} f_{n,k} v^k . \qquad (27)$$

Similarly to Eqs (*25*)–(*27*), using Eq. (*24*) instead of Eq. (*22*), we derive

$$g(x,y) = \sum_{n=0}^{\infty}\sum_{k=0}^{\infty} g_{n,k} y^k / x^{(n+k+1)/2} , \qquad (28)$$

further

$$\begin{aligned} g_{0,2k+1} &= -(-2)^{-k}/(k!(2k+1)) \quad \text{for } k \geq 0, \quad g_{0,2k} = 0 \quad \text{for } k > 0, \\ g_{n+1,1} &= -(n+1)g_{n,0}/2 \quad \text{for } n \geq 0, \quad g_{n,2} = -(n+1)g_{n-1,1}/4 \quad \text{for } n > 0, \quad (29) \\ g_{n+1,k+1} &= -((n+k+1)g_{n,k}/2 + g_{n,k-2}/2)/(k+1) \quad \text{for } k > 1, n \geq 0, \end{aligned}$$

and

$$(\pi / 2)^{1/2} P_n(v) + Q_n(v) \exp(-v^2 / 2) - (\pi / 2)^{1/2} \operatorname{erf}(v / 2^{1/2}) P_n(v) = \sum_{k=0}^{\infty} g_{n,k} v^k, \quad (30)$$

where erf $(x) = 1 - \operatorname{erfc}(x) = (2/\pi^{1/2}) \sum_{n=0}^{\infty} x^{2n+1}(-1)^n / (n!(2n+1))$. Further, $g_{n,0} = f_{n,0}$ and $g_{n,1} = f_{n,1}$. Now we set

$$P_n(v) = \sum_{k=0}^{3n} p_{n,k} v^k, \quad Q_n(v) = \sum_{k=0}^{3n-1} q_{n,k} v^k \quad (31)$$

with $p_{n,k} = 0$ for $n + k$ odd and $q_{n,k} = 0$ for $n + k$ even. Considering the parity of the polynomials $P_n$ and $Q_n$ and of the erf function, it immediately follows from Eqs (*30*) and (*31*) that

$$p_{n,k} = (2 / \pi)^{1/2} g_{n,k} \quad \text{for } n + k \text{ even}, \quad (32)$$

and from Eqs (*27*) and (*31*)

$$q_{n,0} = f_{n,0} \quad \text{for } n \text{ odd}. \quad (33)$$

Since $(\mathrm{d}^n(\exp(v^2/2) \operatorname{erfc}(v/2^{1/2}))/\mathrm{d}v^n)_{v=0} = n!(-1)^n 2^{-n/2}/\Gamma(n/2 + 1)$, by Eq. (*20*) it follows that $R_{2n}(0) = (2n)!2^{-n}/n!$ and $S_{2n+1}(0) = -n!2^n$, which allows to calculate the values $p_{n,0}$ and $q_{n,0}$ using equations following Eq. (*21*) and then the values $g_{n,0} = f_{n,0}$ using Eqs (*32*) and (*33*). At this and in using the recursive formula (*29*), a great loss of accuracy occurs at larger $n$ or $k$, so that it is worth converting the calculation to integers to perform it exactly by multiple-precision integer arithmetic. For this purpose, we set

$$g_{n,k} = b_{n,k}(-1)^k (\pi / 2)^{1/2} / (k! 2^{(3n-k)/2} \Gamma((3n - k) / 2 + 1)). \quad (34)$$

With this substitution, one finds

$$b_{n,0} = a_{n,3n} + \sum_{k=1}^{n-1} (-1)^k 3n(3n-2)\ldots(3n-2k+2) a_{n-k,3n-2k}, \quad (35)$$

$b_{0,k} = 1$, and

$$b_{n,k} = (3n-k)(n+k-1)b_{n-1,k-1}/2 + (k-1)(k-2)b_{n-1,k-3}/2 \quad \text{for } k > 0. \qquad (36)$$

It follows that $b_{1,k} = 1$, $b_{2,k} = k + 4$, $b_{3,k} = k^2 + 19k + 28$, $b_{4,k} = k^3 + 61k^2 + 394k + 160$, and so forth.

From Eqs (*27*), (*32*), and (*23*) and considering the parity of the terms involved, for $n + k$ odd, it follows further that $q_{n,k} = \sum_{j=0}^{k} 2^{-j/2} g_{n,k-j}/\Gamma(j/2+1)$ or

$$q_{n,k} =$$
$$= (\pi/2)^{1/2} \sum_{j=0}^{k} (-1)^j b_{n,j} / (j!2^{(3n+k)/2-j} \Gamma((3n-j)/2+1)\Gamma((k-j)/2+1)). \qquad (37)$$

Now, using Eq. (*6.1.18*) of ref.[4]

$$(3n)!q_{n,k} =$$
$$= \sum_{j=0}^{k} (-1)^j \binom{3n}{j} b_{n,j} 2^{(3n-1-k)/2} \Gamma((3n-1-j)/2+1)/\Gamma((k-j)/2+1). \qquad (38)$$

Since the leading term of $S_{3n}(v)$ is $-v^{3n-1}$ and that of $R_{3n}(v)$ is $v^{3n}$, using the equations following Eq. (*21*) and Eqs (*31*), (*32*), and (*34*), we obtain $q_{n,3n-1} = -p_{n,3n} = -(2/\pi)^{1/2} g_{n,3n} = (-1)^{n-1} b_{n,3n}/(3n)!$, so that using Eq. (*38*) with $k = 3n - 1$ yields

$$\sum_{j=0}^{3n} (-1)^j \binom{3n}{j} b_{n,j} = 0. \qquad (39)$$

Suppose that for $j \geq 0$, $b_{n-1,j}$ are given by a polynomial of $j$ of a degree at most $n - 2$ (an induction proposal valid for $n = 2$). Then, using Eq. (*36*), $b_{n,j}$ for $j > 0$ are given by a polynomial of $j$ of a degree at most $n - 1$, since the terms with $j^n$ cancel. Then Eq. (*39*) can be valid only when $b_{n,0}$ is given by the same polynomial as $b_{n,j}$. This gives another method to calculate $g_{n,0}$: spread the equality $b_{1,k} = 1$ down to $k = 3 - 3n$ and successively use the recursion (*36*) with any integer $k$ and then Eq. (*34*). Also, Eq. (*36*) can be used for successive expressing $b_{n,k}$ for individual $n$'s as polynomials of $k$.

Note that $b_{n,j}\Gamma((3n-1-j)/2+1)/\Gamma((k-j)/2+1)$ is a polynomial of $j$ of a degree lower than $3n$. So, spreading the summation in Eq. (*38*) up to $3n$ gives zero, hence

$$(3n)!q_{n,k} = \\ = \sum_{j=k+1}^{3n} (-1)^{j+1} \binom{3n}{j} b_{n,j} 2^{(3n-1-k)/2} \Gamma((3n-1-j)/2+1)/\Gamma((k-j)/2+1). \quad (40)$$

Here the summation terms for $j = k + 2$, $k + 4$, $k + 6$, and so forth are zero. Equation (*40*) says the following: when the asymptotic development of $\exp(y^2/(2x))\,\mathrm{erfc}(y/(2x)^{1/2})$ (see ref.[4], Eq. (*7.1.23*)) is used for a large $y$ in Eq. (*21*), the whole $Q_n(y/x^{1/2})$ cancels and only negative powers of $y$ are retained. Hence, great loss of accuracy occurs at large values of $y$ making Eq. (*21*) unsuitable for a calculation. Equations (*28*) and (*23*) should be used instead. For calculating $(3n)!q_{n,k}$, either of Eqs (*38*) or (*40*) can be used with integer arithmetic. For larger $n$, multiple precision should be used due to the great loss of accuracy.

With $I(\omega) = \tau_c \mathrm{Re}[f(\omega_p^2\tau_c^2, \mathrm{i}(\omega-\omega_0)\tau_c)]/\pi$, the asymptotic development reads

$$\begin{aligned} I(\omega) = {} & (2\pi)^{-1/2}\omega_p^{-1} \exp(-z^2/2)[1 + (2/\pi)^{1/2}((1/3 - z^2/6)\exp(z^2/2) - \\ & - (z/2 - z^3/6)\,D(z))/(\omega_p\tau_c) + (1/12 - 3z^2/8 + z^4/6 - z^6/72)/(\omega_p\tau_c)^2 + \\ & + (2/\pi)^{1/2}((4/135 - 241z^2/1080 + 293z^4/2160 - 13z^6/648 + \\ & + z^8/1296)\exp(z^2/2) - (z/8 - 47z^3/144 + 37z^5/240 - z^7/48 + \\ & + z^9/1296)\,D(z))/(\omega_p\tau_c)^3 + (1/288 - 5z^2/32 + 347z^4/1152 - 617z^6/4320 + \\ & + 23z^8/960 - z^{10}/648 + z^{12}/31104)/(\omega_p\tau_c)^4 + ....] , \end{aligned} \quad (41)$$

where $z = (\omega - \omega_0)/\omega_p$, and $D(z) = \int_0^z \exp(t^2/2)\,\mathrm{d}t$ is the Dawson integral. Taking just the first term (the unity) in the brackets yields the parent non-narrowed Gaussian shape back.

The asymptotic development for large $|\omega - \omega_0|$ (*i.e.*, large $y$) is sought in the form

$$f(x,y) = \sum_{n=0}^{\infty}\sum_{k=1}^{\infty}(-1)^{n+k+1} f_{n,k} x^n / y^k . \qquad (42)$$

With Eq. (*22*), we obtain

$$f_{0,1} = 1, \quad f_{n,k} = nf_{n,k-1} + (k-2)f_{n-1,k-2} \qquad (43)$$

when setting $f_{n,k} = 0$ for $n < 0$ and for $k \le 0$. Then $f_{0,k} = 0$ for $k > 1$, $f_{n,k} = 0$ for $k \le 2n$, $f_{1,k} = 1$ for $k > 2$, $f_{2,k} = 2^{k-2} - k$ for $k > 4$, $f_{3,k} = 3^{k-2}/2 - (k+1)2^{k-3} + (k^2 - k + 1)/2$ for $k > 6$, and, for $n > 1$, $f_{n,2n+1} = (2n-1)(2n-3)....\times 5 \times 3$ and $f_{n,2n+2} = n(2n+1)(2n-1).... \times 7 \times 5$. Herefrom

$$I(\omega) = \tau_c[x/y^4 + (10x^2 - x)/y^6 + (105x^3 - 56x^2 + x)/y^8 + + (1260x^4 - 1918x^3 + 246x^2 - x)/y^{10} + ....]/\pi , \qquad (44)$$

$x = \omega_p^2\tau_c^2$, $y = (\omega - \omega_0)\tau_c$. This is exactly what is obtained by expanding Eq. (*6a*) or (*14*) in negative powers of $y$. For a numerical calculation, Eq. (*14*) (or (*6a*)) is more suitable since it is convergent (not semidivergent like Eq. (*44*)); moreover, Eq. (*14*) involves positive terms only, so that no loss of accuracy occurs.

For large $x$, the large $y$ asymptotic development (*44*) should be expressed in terms of the variable $y/x^{1/2}$ instead of $y$. Transforming Eq. (*44*) in this way yields only negative powers of $x$ in the numerator, so that the transformed Eq. (*44*) gives the asymptotic development for both $y/x^{1/2}$ (*i.e.*, $|\omega - \omega_0|/\omega_p$) and $x$ large. This is exactly what is obtained by the asymptotic development of $\exp(y^2/(2x))\,\mathrm{erfc}(y/(2x)^{1/2})$ for large $y/x^{1/2}$ in Eq. (*21*).

*The Anisotropic Case*

Fast segmental motions of a polymer chain are rather anisotropic, so that the second-order spherical-harmonics autocorrelation function $G(t)$, determining the $T_1$, $T_2$, and NOE values, is multiexponential (see, *e.g.*, ref.[7], Eq. (*7*)). As a consequence, the simple Anderson approach as such cannot be used for this case. Although the spectral autocorrelation function, $\varphi_{\Delta\omega}(\tau)$, is generally different from the second-order spherical-harmonics one, $G(t)$, it seems reasonable to use a multiexponential function for the spectral autocorrelation one as well, at least as an approximation. The multi-exponential spectral autocorrelation function reads

$$\varphi_{\Delta\omega}(\tau) = \sum_{i=1}^{r} \alpha_i \exp(-|\tau|/\tau_i), \quad \sum_{i=1}^{r} \alpha_i = 1 \tag{45}$$

with a finite or infinite $r$. Then the Fourier transform $\varphi(\tau)$ of the narrowed Gaussian line becomes

$$\varphi(\tau) = \prod_{i=1}^{r} \exp(\alpha_i \omega_p^2 \tau_i^2 [1 - |\tau|/\tau_i - \exp(-|\tau|/\tau_i)]). \tag{46}$$

When all $\tau_i$ except for a single one ($\tau_1$) allow for the extreme narrowing approximation, we have

$\varphi(\tau) = \exp(\alpha_1 \omega_p^2 \tau_1^2 [1 - |\tau|/\tau_1 - \exp(-|\tau|/\tau_1)]) \times \exp(-\omega_p^2 |\tau| \sum_{i=2}^{r} \alpha_i \tau_i)$, or, if we set $\alpha = \alpha_1$, $\tau_c = \tau_1$ and introduce an average fast correlation time $\tau_f = \sum_{i=2}^{r} \alpha_i \tau_i / (1 - \alpha)$,

$$\varphi(\tau) = \exp(\alpha \omega_p^2 \tau_c^2 [1 - |\tau|/\tau_c - \exp(-|\tau|/\tau_c)]) \times \exp(-(1-\alpha)\omega_p^2 \tau_f |\tau|). \tag{47}$$

We see that the narrowed shape is the convolution of the Anderson shape originating from the slow correlation time $\tau_c$ and the parent second moment reduced by the factor $\alpha$, *i.e.*, $\alpha\omega_p^2$, with the Lorentzian shape originating from the average fast correlation time $\tau_f$ and the second moment reduced by the factor $1 - \alpha$, *i.e.*, $(1 - \alpha)\omega_p^2$.

Setting $x = \omega_p^2 \tau_c(\alpha\tau_c + (1 - \alpha)\tau_f)$, $v = (1 - \alpha)\omega_p^2 \tau_c \tau_f / x$, and $y = (\omega - \omega_0)\tau_c$, and inverting Fourier transform similarly as above, we obtain using the substitution $\alpha\omega_p^2 \tau_c^2 \exp(-\tau/\tau_c) = z$

$$I(\omega) = \tau_c \,\mathrm{Re}[((1-v)x)^{-x-\mathrm{i}y} \exp((1-v)x) \gamma(x + \mathrm{i}y, (1-v)x)] / \pi \tag{48}$$

and

$$I(\omega) = \tau_c \,\mathrm{Re}[\sum_{n=0}^{\infty} ([(1-v)x]^n / \prod_{k=0}^{n} (x + \mathrm{i}y + k))] / \pi. \tag{49}$$

Avoiding the complex numbers arithmetic by introducing Eq. (*11*) into Eq. (*49*) and summing up with respect to $j$ at constant $i$, we obtain as above

$$I(\omega) = \tau_c[\sum_{n=0}^{\infty}([(1-v)x]^n U_n(x,v) / \prod_{k=0}^{n}((x+k)^2 + y^2))] / \pi , \qquad (50)$$

where $U_n(x, v)$ are polynomials of $x$ and $v$, again with positive integer coefficients. There is $U_0 = vx$, $U_1 = v(v + 1)x^2 + 3vx + 1$, $U_2 = v(v + 1)^2x^3 + v(10v + 8)x^2 + (24v + 2)x + 12$, $U_3 = v(v + 1)^3x^4 + v(v + 1)(21v + 15)x^3 + (135v^2 + 100v + 3)x^2 + (300v + 42)x + 180$, $U_4 = v(v + 1)^4x^5 + v(v + 1)^2(36v + 24)x^4 + (448v^3 + 700v^2 + 268v + 4)x^3 + (2352v^2 + 1692v + 96)x^2 + (5040v + 904)x + 3360$, and so forth, generally $U_n = v(v + 1)^n x^{n+1} + v(v + 1)^{n-2}n((2n + 1)v + n + 2)x^n + (v + 1)^{n-4}n((2n - 1)n^2v^3 + (2n - 1)(3n^2 + 7n - 1)v^2/3 + (3n^3 + 10n^2 + 15n - 10)v/6 + 1)x^{n-1} + (v + 1)^{n-6}n(n - 1)(n(2n - 1)^2(n - 1)v^4/3 + (n - 1)(12n^3 + 26n^2 - 31n + 6)v^3/6 + (2n^4 + 7n^3 + 7n^2 - 28n + 12)v^2/2 + (n^4 + 5n^3 + 17n^2 + 37n - 54)v/6 + n + 4)x^{n-2} + ...$ . Other coefficients should again be obtained by numerical summation with respect to $j$ expanding the factor $(1 - v)^{j-i}$ by the binomial theorem and summing up the coefficients at each particular power of $v$. Note that $U(x, 0) = U(x)$.

To consider the asymptotic development of Eq. (*49*) for large $(1 - v)x$, we realize that $I(\omega) = \tau_c \mathrm{Re}[f((1 - v)x, vx + \mathrm{i}y)]/\pi$ with the function $f$ defined by Eq. (*15*). The asymptotic development can be calculated using either Eq. (*21*) or Eqs (*28*) and (*23*). One should keep in mind, however, that $y$ in Eq. (*21*) or Eqs (*28*) and (*23*) is not pure imaginary now, but complex with positive real part, so that odd powers of $y$ should be considered as well.

## RESULTS AND DISCUSSION

Figure 1 shows the partially narrowed line shapes for the case of the slow motion (*i.e.*, for $\tau_c \geq 0.5/\omega_p$) compared with the parent Gaussian line; $(2\pi)^{1/2}\omega_p I(\omega)$ values are plotted *versus* $(\omega - \omega_0)/\omega_p$. Scaling with $\omega_p$ makes the line shapes independent of the width of the parent Gaussian line. The narrowing is striking. It is also seen that for $|\omega - \omega_0| > 2.7\omega_p$, the wings grow with increasing narrowing. The reason is that the $(\omega - \omega_0)^{-4}$ wing decrease in the narrowed lines is slower than the exponential one in the parent Gaussian line. In fact, the curves in Fig. 1 must intersect at least twice, since both the integral intensity and the second moment do not change during narrowing. Figure 2 shows the first-order term (multiplied by $(2\pi)^{1/2}\omega_p^2\tau_c$, the full curve) and the second-order term (multiplied by $(2\pi)^{1/2}\omega_p^3\tau_c^2$, the dotted curve) of the asymptotic development for large $\tau_c$ of the narrowed

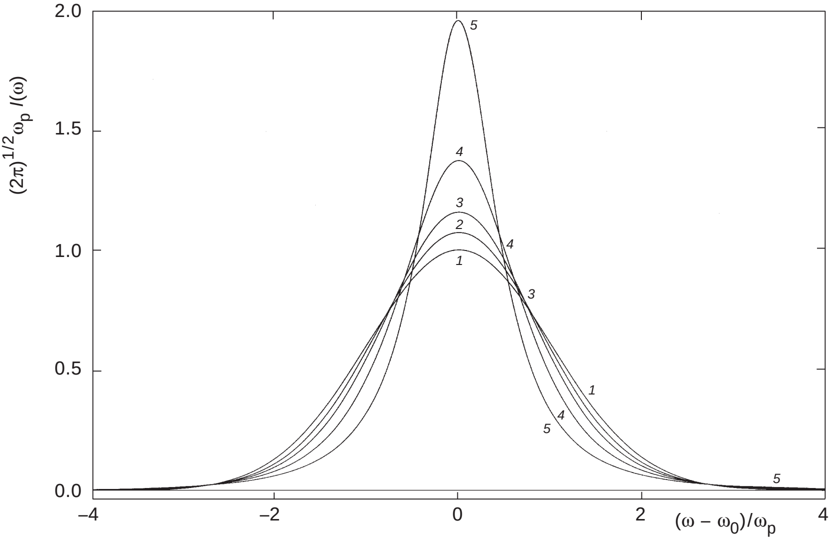


FIG. 1
Plots *versus* $(\omega - \omega_0)/\omega_p$ of $(2\pi)^{1/2}\omega_p\,I(\omega)$ values for the partially narrowed Gaussian lines and the Gaussian line. The $\omega_p\tau_c$ values: *1* ∞ (the Gaussian line); *2* 4; *3* 2; *4* 1; *5* 1/2

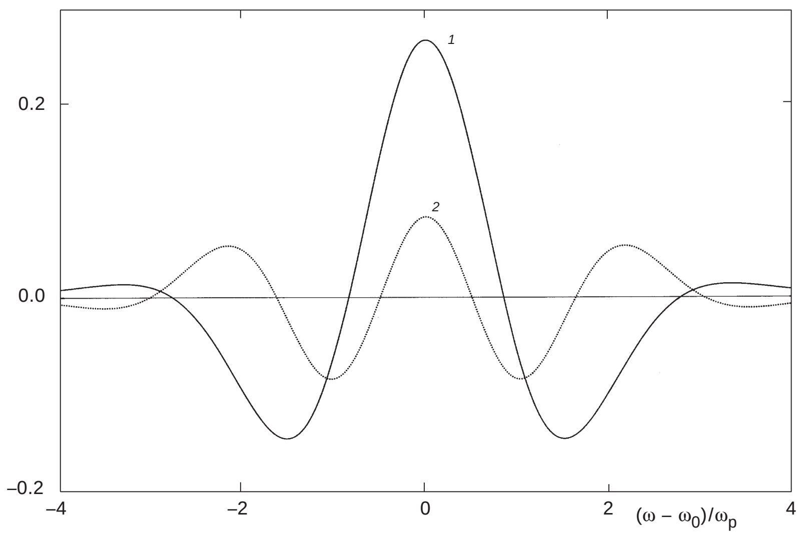


FIG. 2
Plots *versus* $(\omega - \omega_0)/\omega_p$ of the first- and second-order terms of the asymptotic development for the case of the slow motion (large $\tau_c$) of the partially narrowed line shapes. *1* (the full curve): the first-order term multiplied by $(2\pi)^{1/2}\,\omega_p^2\tau_c$; *2* (the dotted curve): the second-order term multiplied by $(2\pi)^{1/2}\,\omega_p^3\tau_c^2$

line shape. The second-order term root at $|\omega - \omega_0|/\omega_p = 3.0179$ is close to the first-order one at 2.7656; this may be the reason why all curves in Fig. 1 intersect nearly in the same point $|\omega - \omega_0|/\omega_p \doteq 2.7$.

Figure 3 shows the partially narrowed line shapes for the case of the fast motion (*i.e.*, for $\tau_c \leq 1/\omega_p$) compared with the Lorentzian line of extreme narrowing; $\pi\omega_p^2\tau_c I(\omega)$ values are plotted *versus* $(\omega - \omega_0)/(\omega_p^2\tau_c)$. Due to abscissa scaling with $\tau_c$, the lines seemingly broaden with increasing narrowing. This only means that, with the $\tau_c$ decrease, the narrowing proceeds more slowly than expected from the extreme narrowing approximation. The $(\omega - \omega_0)^{-4}$ wing decrease is apparent with curves with $\omega_p\tau_c$ of 1 and 1/2. It turns out that the partially narrowed lines are narrower than the lines in both limiting cases of the Gaussian line of the second moment of $\omega_p^2$ and the Lorentzian line of the half-width of $2\omega_p^2\tau_c$. The increase in the central intensity of the narrowed line, compared with the closer of the two limiting cases, is less than 50.19%; the greatest increase appears at $\omega_p\tau_c = (2/\pi)^{1/2} = 0.7979$.

For detecting the partially narrowed lines in real NMR spectra, it is worth having their comparison with Gaussian and Lorentzian lines with optimized widths and integral intensities. Least-squares optimization is

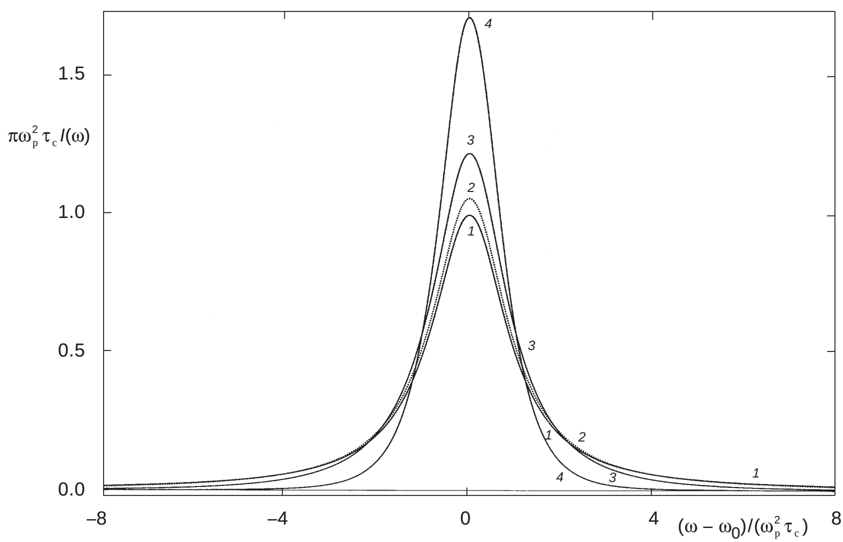


FIG. 3
Plots *versus* $(\omega - \omega_0)/(\omega_p^2\tau_c)$ of $\pi\omega_p^2\tau_c I(\omega)$ values for the partially narrowed Gaussian lines and the Lorentzian line. The $\omega_p\tau_c$ values: *1* 0 (the Lorentzian line); *2* (the dotted curve) 1/4; *3* 1/2; *4* 1

achieved by minimizing $\int_{-\infty}^{\infty}(I(\omega)-I_0L((\omega-\omega_0)/w)/w)^2\,\mathrm{d}\omega$, where $w$ and $I_0$ are the line width and integral intensity. To find optimum $w_\mathrm{m}$, it is necessary to maximize $w^{1/2}J(w)$, where $J(w)=\int_{-\infty}^{\infty}I(\omega)L((\omega-\omega_0)/w)\,\mathrm{d}\omega/w$. For Gaussian $L(x)=(2\pi)^{-1/2}\omega_\mathrm{p}^{-1}\exp(-(x/\omega_\mathrm{p})^2/2)$, $J(w)=\tau_\mathrm{c}\int_0^{\infty}\exp(\omega_\mathrm{p}^2\tau_\mathrm{c}^2[1-\tau-\exp(-\tau)-w^2\tau^2/2])\,\mathrm{d}\tau/\pi$. This expression was calculated by the Euler–Maclaurin summation formula (Eq. (*25.4.7*) of ref.[4]) with $h=1/(128\omega_\mathrm{p}\tau_\mathrm{c})$ and $k=3$, neglecting the remainder $R_6$. With large $\omega_\mathrm{p}\tau_\mathrm{c}$, the asymptotic formula $J(w)=(2\pi(1+w^2))^{-1/2}\omega_\mathrm{p}^{-1}(1+\sum_{n=1}^{\infty}\sum_{k=0}^{n-1}h_{n,k}(-w^2)^k/[2^{3n/2-k}\Gamma(3n/2-k+1)\omega_\mathrm{p}^n\tau_\mathrm{c}^n(1+w^2)^{3n/2}])$ can be used, where $h_{n,k}$ are the coefficients of the interpolation formula for $b_{n,k}$ in the form $b_{n,k}=h_{n,0}+kh_{n,1}+k(k-2)h_{n,2}+\ldots+k(k-2)(k-4)\ldots(k-2n+4)h_{n,n-1}$. Matching both formulae at $\omega_\mathrm{p}\tau_\mathrm{c}=4$ and several values of $w$ checks their correctness. The first terms of the asymptotic formula match with what is obtained by the analytical integration of $J(w)$ using Eq. (*41*). For Lorentzian $L(x)=\omega_\mathrm{p}^2\tau_\mathrm{c}/(\pi(\omega_\mathrm{p}^4\tau_\mathrm{c}^2+x^2))$, $J(w)$ was calculated using the right-hand side of Eq. (*49*) with $x=(1+w)\omega_\mathrm{p}^2\tau_\mathrm{c}^2$, $v=w/(1+w)$, and $y=0$. Then the optimum $I_0$ equals $w_\mathrm{m}J(w_\mathrm{m})/\int_{-\infty}^{\infty}L^2(x)\,\mathrm{d}x$. For the Gaussian shape, $\int_{-\infty}^{\infty}L^2(x)\,\mathrm{d}x$ equals $\pi^{-1/2}/(2\omega_\mathrm{p})$, for the Lorentzian one $1/(2\pi\omega_\mathrm{p}^2\tau_\mathrm{c})$.

A comparison of the partially narrowed lines with the Gaussian lines optimized by the least-squares is shown in Fig. 4 and with the Lorentzian ones in Fig. 5. For $\omega_\mathrm{p}\tau_\mathrm{c}$ of 4, 2, 1, and 0.5, the Gaussian $w_\mathrm{m}$ values (*i.e.*, the ratios of the optimized Gaussian widths to the parent Gaussian width) are 0.9293, 0.8586, 0.7210, and 0.4935; the optimized integral intensities are 0.9876, 0.9737, 0.9426, and 0.8791, respectively. For $\omega_\mathrm{p}\tau_\mathrm{c}$ of 0.25, 0.5, and 1, the Lorentzian $w_\mathrm{m}$ values (*i.e.*, the ratios of the optimized Lorentzian widths to the Lorentzian width in the extreme narrowing approximation) are 0.9880, 0.9024, and 0.6616; the optimized integral intensities are 1.0509, 1.1269, and 1.1984, respectively. At $\omega_\mathrm{p}\tau_\mathrm{c}=1/4$, both compared lines nearly match. It is seen that the main difference found in the line comparison is the increasing wing intensity in proceeding narrowing. This becomes much more striking when a comparison with Gaussians and Lorentzians of the same central intensities and half-widths is made. Here the deviations near the line center are small and those in wings very large. For $\omega_\mathrm{p}\tau_\mathrm{c}$ of 4, 2, 1, and 0.5, the ratios of the Gaussian widths to the parent Gaussian width are 0.9116, 0.8228, 0.6529, and 0.4067; the integral intensities are 0.9774, 0.9519, 0.8952, and 0.7943, respectively. For $\omega_\mathrm{p}\tau_\mathrm{c}$ of 0.25, 0.5, and 1, the ra-

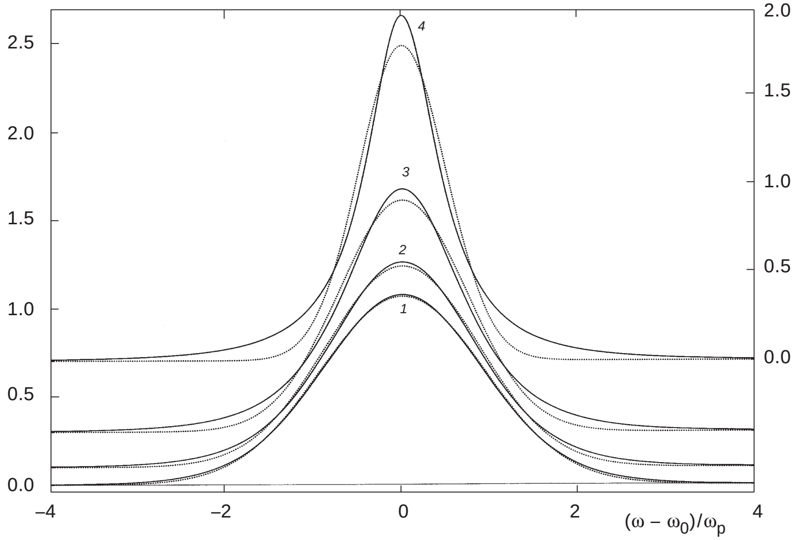


FIG. 4
A comparison with the least-squares optimized Gaussian lines (dotted curves) of the partially narrowed lines (full curves). $(2\pi)^{1/2}\omega_p\, I(\omega)$ values *versus* $(\omega - \omega_0)/\omega_p$ are plotted. The $\omega_p\tau_c$ values: *1* 4; *2* 2; *3* 1; *4* 1/2

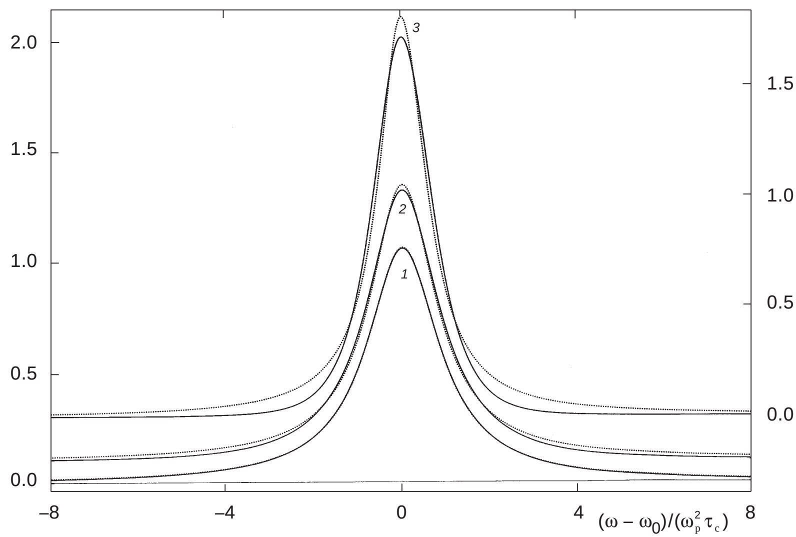


FIG. 5
A comparison with the least-squares optimized Lorentzian lines (dotted curves) of the partially narrowed lines (full curves). $\pi\omega_p^2\tau_c I(\omega)$ values *versus* $(\omega - \omega_0)/(\omega_p^2\tau_c)$ are plotted. The $\omega_p\tau_c$ values: *1* 1/4; *2* 1/2; *3* 1

tios of the Lorentzian widths to the Lorentzian width in the extreme narrowing approximation are 0.9964, 0.9576, and 0.7688; the integral intensities are 1.0568, 1.1722, and 1.3210, respectively.

A comparison is shown of a spectrum of poly(2-ethylhexyl acrylate)-*block*-poly(acrylic acid) micelles in deuterated water[1] with a synthesis of eight (plus two to catch artifact lines of residual ordinary water lying beyond the shown part) Gaussian (Fig. 6) or Lorentzian (Fig. 7) lines, where the line widths and integral intensities are optimized by least squares. Line overlapping and the asymmetry of marginal lines at 2.385 and 0.856 ppm to some extent mask effects expected on the basis of Figs 4 and 5. Nevertheless, it is clearly seen, that the Gaussian shape is too weak and the Lorentzian one too strong in wings and that a shape with intermediate wings like the Anderson one should considerably improve the agreement between the synthetic and actual spectra.

Limitations imposed by using an approximate Gaussian shape for the parent rigid-lattice spectrum and the approximate exponential function for the spectral autocorrelation function should be briefly discussed. Testing dipolar interactions in the rigid cubic lattice revealed some deviations of

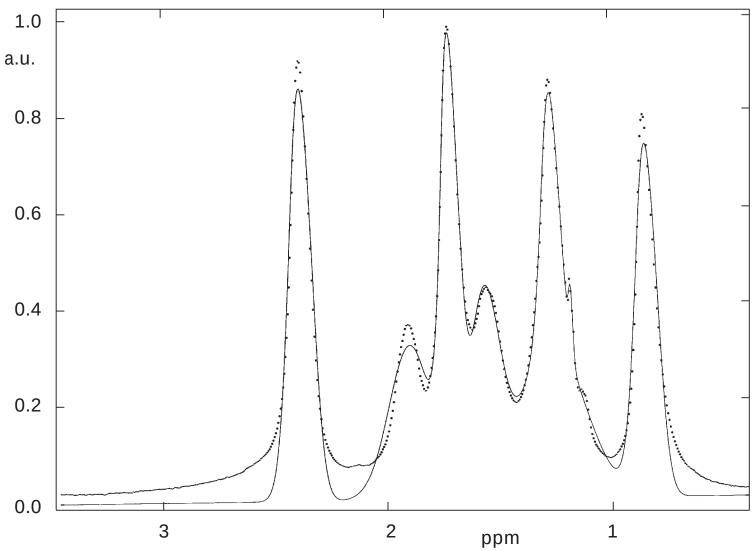


FIG. 6
A comparison of a spectrum of poly(2-ethylhexyl acrylate)-*block*-poly(acrylic acid) micelles in deuterated water[1] with a synthetic spectrum of Gaussian lines. Full curve: the synthetic spectrum. Dots: the actual spectrum

the $M_4/M_2^2$ ratio from the Gaussian value of 3; however, it was believed that these were not so important as to make the Gaussian shape grossly incorrect[8]. It turns out that the exact shape is more flat in the center of the line than the Gaussian shape. The necessity of using the Gaussian shape stems primarily from its generality, besides its simplicity. Since, in the extreme narrowing, the resulting line shape is Lorentzian regardless of the rigid-lattice spectrum[3], it may be believed that at least at considerable narrowing (small values of $\omega_p\tau_c$), the differences of the calculated narrowed shape from the exact one are negligible.

Motions effecting band narrowing are jump-like Markovian processes (molecular collisions in a solution, three- and four-bond motions[7] in a flexible polymer chain). For such processes, the correlation function is exponential (ref.[3], Eq. (*35*)), or multiexponential when the motion is complicated. A multiexponential correlation function with a narrow distribution of correlation times (say, within one half decade) can be well approximated with a single-exponential correlation function in view of the low resolution of the integral transform inversion. The case when, in addition to one correlation time causing partial narrowing, some correlation

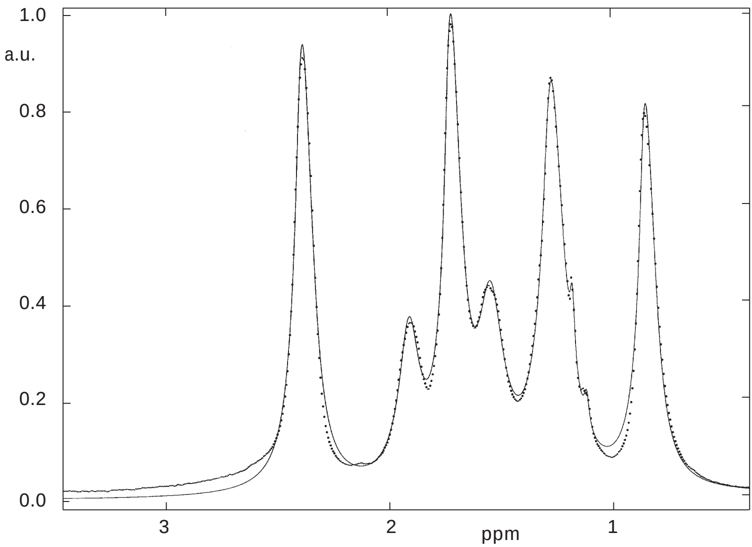


FIG. 7
A comparison of a spectrum of poly(2-ethylhexyl acrylate)-*block*-poly(acrylic acid) micelles in deuterated water[1] with a synthetic spectrum of Lorentzian lines. Full curve: the synthetic spectrum. Dots: the actual spectrum

times causing extreme narrowing appear is considered in Part "The Anisotropic Case". When some nearly "rigid" correlation times appear, the convolution with the Gaussian shape is desirable. Here, however, the deviations of the parent shape from the Gaussian one may become relevant.

The situation can be visualized in a simple model of spin flipping in a rigid spin system. When every interacting spin causes a splitting small compared to the spectral line width, the Gaussian shape provides a good approximation to the parent line shape in the absence of flipping (it is exact when spins are infinite in number, each causing infinitesimal splitting). When all spins flip at the same rate, the spectral autocorrelation function is single-exponential. When various spins flip with different rates, a multi-exponential spectral autocorrelation function results. When few of interacting spins cause a splitting too large to allow for the Gaussian approximation, the parent line shape may be well approximated by convolution of the multiplet resulting from them with the Gaussian shape resulting from the other spins. The shape narrowed by flipping then results from the convolution of the narrowed members of the parent convolution. The narrowed shape of a multiplet consists of several Lorentzian lines, which contain the dispersion component as well when lying off the center of the parent line[3]. For several spins, the shape can be built on as convolution of shapes resulting from individual spins. The convolution of the Lorentz and Anderson shapes is treated in Part "The Anisotropic Case", the convolution of the Lorentz dispersion component shape with the Anderson shape may be found similarly.

Clearly, the motional narrowing is much more complicated than the spin-flipping one due to the orientational dependence of the splitting magnitude. Nevertheless, the previous paragraph may serve as a good hint for seeking a route solving situations where both the Anderson shape and its convolution with the Lorentz shape lack sufficient accuracy to fit an actual partially narrowed line shape.

*The financial support by the Grant Agency of the Academy of Sciences of the Czech Republic (grant No. K2050602/12) is gratefully acknowledged.*

## REFERENCES

1. Kříž J., P1eštil J., Tuzar Z., Pospíšil H., Brus J., Jakeš J., Masař B., Vlček P., Doskočilová D.: *Macromolecules* **1999**, *32*, 397.
2. Anderson P. W., Weiss P. R.: *Rev. Mod. Phys.* **1953**, *25*, 269.
3. Anderson P. W.: *J. Phys. Soc. Jpn.* **1954**, *9*, 316.

4. Abramowitz M., Stegun I. A.: *Handbook of Mathematical Functions*. Dover, New York 1965.
5. Furch R.: *Z. Phys.* **1939**, *112*, 92.
6. a) Tricomi F. G.: *Boll. Unione Mat. Ital.* **1950**, *4*, 341; b) Tricomi F. G.: *Math. Z.* **1950**, *53*, 136; c) Tricomi F. G.: *Ann. Math. Pure Appl.* **1951**, *28*, 263; d) Tricomi F. G.: *J. Anal. Math.* **1951**, *1*, 209.
7. Jakeš J.: *Collect. Czech. Chem. Commun.* **2000**, *65*, 1537.
8. Abragam A.: *The Principles of Nuclear Magnetism*, p. 113. Clarendon Press, Oxford 1962.